Forest liming in the face of climate change: the implications of restorative liming on soil organic carbon in mature German forests

Oliver van Straaten[1], Larissa Kulp[1], Guntars O. Martinson[2], Dan Paul Zederer[1, 3], Ulrike Talkner[1*]

1. Northwest German Forest Research Institute, Grätzelstr. 2, D-37079 Göttingen, Germany
2. Soil Science of Tropical and Subtropical Ecosystems, University of Göttingen, Büsgenweg 2, D-37077 Göttingen, Germany
3. Saxon State Office for Environment, Agriculture and Geology, Department of Agriculture, Waldheimer Str. 219, D-01683 Nossen, Germany

* Correspondence email: ulrike.talkner@nw-fva.de

Abstract

Forest liming is a management tool that has and continues to be used extensively across northern Europe to counteract acidification processes from anthropogenic sulfur and nitrogen (N) deposition. In this study, we quantified how liming affects soil organic carbon (SOC) stocks and attempt to disentangle the mechanisms responsible for the often-contrasting processes that regulate net soil carbon (C) fluxes. Using a paired-plot experimental design we compared SOC stocks in limed plots with adjacent unlimed control plots at 28 experimental sites to 60-cm soil depth in mature broadleaf and coniferous forests across Germany. Historical soil data from a subset of the paired experiment plots was analyzed to assess how SOC stocks in both control and limed plots had changed between 1990 and 2019.

Overall, we found that forest floor C stocks have been accumulating over time in the control plots. Liming however largely offset organic layer buildup in the L/O_f layer and forest floor C stocks remained unchanged over time in the limed plots. This, in turn meant that nutrients remained mobile and were not bound in soil organic matter complexes. Results from the paired plot analysis showed that forest floor C stocks were significantly lower in limed plots than the control (-34 %, -8.4 ± 1.7 Mg C ha^{-1}), but did not significantly affect SOC stocks in the mineral soil, when all sites are pooled together. In the forest floor layers, SOC stocks exhibited an exponential decrease with increasing pH, highlighting how lime-induced improvements in the biochemical environment stimulate organic matter (OM) decomposition. Nevertheless, for both forest floor and mineral soils, the magnitude and direction of the belowground C changes hinged directly on the inherent site characteristics, namely, forest type (conifer versus broadleaf), soil pH, soil texture and the soil SOC stocks. On the other hand, SOC stock decreases were often offset by other processes that fostered C accumulation, such as improved forest productivity or increased carbon stabilization, which correspondingly translated to an overall variable response by SOC stocks, particularly in the mineral soil.

Lastly, we measured soil carbon dioxide (CO_2) and soil methane (CH_4) flux immediately after a re-liming event at three of the experimental sites. Here, we found that (1) liming doubles CH_4 uptake in the long-term, (2) highlighted that soil organic matter mineralization processes respond quickly to liming, even though the duration and size of the CO_2 flush varied between sites, and (3) lime-derived CO_2 contributed very little to total CO_2 emissions over the measurement period (determined using stable isotope approaches).

1. Introduction

Millions of hectares of forest have been limed in Germany and across northern Europe over the last few decades to counteract soil acidification processes derived from anthropogenic sulfur (S) and nitrogen (N) deposition. Soil acidification is responsible for hindering organic matter decomposition processes and concomitantly immobilizing nutrients and carbon (Shen et al., 2021).The application of lime on acidic soils, as either calcium carbonate ($CaCO_3$) or dolomite ($CaMg(CO_3)_2$) elicits a strong biochemical response by lowering soil acidity, reducing both aluminum (Al) and manganese toxicity and increasing the soil's buffering capacity. These changes subsequently drive a cascade of ecosystem responses, with implications on soil fertility, forest productivity, stand vitality and litter decomposition (Derome et al., 2000, Kreutzer, 1995), which in turn correspondingly affect the ecosystem carbon (C) balance (Melvin et al., 2013; Persson et al., 2021) and soil greenhouse gas (GHG) budgets. The direction and magnitude of ecosystem responses to liming depends on numerous factors, including: (1) the inherent soil characteristics of the site (soil acidity, soil texture, the chemical make-up of the forest floor layer), (2) vegetation characteristics (species distributions, tree density, and stand age), (3) the application of lime (type and quantity of lime, and frequency of liming) and (4) the ongoing acidification from recent N and S deposition. In this context, both above- and below-ground carbon stocks have been shown to have quite variable responses to liming (Court et al., 2018; Lundström et al., 2003; Melvin et al., 2013; Persson and Ahlström, 1990; Persson et al., 2021).

While it is broadly reported that liming stimulates soil microbial activity leading to accelerated soil organic matter (SOM) decomposition (Andersson and Nilsson, 2001, Kreutzer, 1995), some studies report either no change in litter and forest floor decomposition (Smolander et al., 1996) or even forest floor organic matter accumulations (Derome et al., 2000; Melvin et al., 2013). Soil organic carbon (SOC) stock gains as a result of liming can be attributed to different drivers. First, earthworm abundance is known to increase after liming (Persson et al., 2021) which, by actively incorporating and binding SOM with the mineral soil improves physical properties, such as soil structure and aggregate stability (Bronick and Lal, 2005). Second, physicochemical properties are also affected. Liming-induced changes in nutrient-stoichiometry may enhance cation mediated cross-linking between SOM compounds and divalent calcium (Ca) or magnesium (Mg) ions (Kalbitz et al., 2000) thereby stabilizing soil carbon. It has also been shown that higher soil Ca availability increases lignin contents in leaf litter which makes litter more recalcitrant and resistant to decomposition (Eklund and Eliasson, 1990; Xing et al., 2021). Third, liming will affect microbial community structure and abundance, which has the potential to create nutrient imbalances (such as phosphorus) on decomposer communities and trees (Melvin et al., 2013) which in turn may decrease microbial breakdown of SOM. Lastly, liming-induced improvements in nutrient availability (Jansone et al., 2020; Long et al., 2015), may increase ecosystem productivity

76 which correspondingly can increase SOM inputs from aboveground (e.g. leaf litter (Lin et al., 2015)) and belowground sources (e.g. root detritus).

78 In this study, we quantified the magnitude of SOC stock changes resulting from forest liming activities, with the explicit intent to better understand the implications of liming on soil organic carbon and forest

80 soil greenhouse gas (GHG) budgets. Given the lack of a consistent direction in which SOC stocks respond to liming as reported in literature, we attempted to disentangle the mechanisms responsible

82 for the often-contrasting processes that regulate net carbon fluxes in the soil. Here, we also assessed liming effects across different time scales, ranging from the immediate effects liming has on soil carbon

84 dioxide (CO_2) production, to methane (CH_4) uptake, to long-term changes in soil carbon stocks measured several decades after liming. The study was implemented at experimental sites in managed

86 mature forests across Germany using both space-for-time substitution and chronosequence approaches.

88 We hypothesized that liming-induced changes in SOC stocks will be most pronounced at the soil surface. More specifically, we expect that there will be significant decreases in the forest floor layer C

90 stock because SOM decomposition will be stimulated by reduced pH levels. However, these C losses will be offset if not exceeded, by significant gains in SOC stocks in the topsoil because of improved

92 ecosystem productivity, increased fine root biomass in the upper mineral soil horizons and increased earthworm activity, which will improve soil structure thereby protecting SOM from mineralization.

94 **2. Methods and Materials**

2.1 Experimental study sites

96 Liming effects on soil organic carbon stocks were determined at 28 liming experiment sites distributed across Germany (Figure A1). All sites consisted of mature forest stands whereby all, except one (HLI

98 2680) were managed, meaning these sites were occasionally selectively harvested. Lime was applied in different forms (dolomite ($CaMg(CO_3)_2$) and calcium carbonate ($CaCO_3$)) and in differing quantities,

100 ranging from a total between 2-9 tons per hectare spread over multiple application dates (Table 1). The last lime application at most sites was typically 20 to 30 years prior to our sampling, and therefore

102 findings reflect the long-term effects liming has on belowground carbon. The experiment was conducted using a paired plot design, where each site consisted of a limed plot adjacent to a control

104 plot which was not limed. In total, for this analysis, we sampled nine sites with European beech (*Fagus sylvatica* L.), two with common oak (*Quercus robur* L.), 16 with Norway spruce (*Picea abies* L. karst.)

106 and one European red pine (*Pinus sylvestris* L.) site. General site characteristics are described in Table 1. At two spruce sites (GOH 155, SEG 244) we only had data from the forest floor layers, and not the

108 mineral soil as soil bulk density data were unavailable. Nitrogen deposition was ascertained from the German Environment Agency (Umweltbundesamt, 2019).

Table 1: Site characteristics and liming details of the 28 experimental sites. Soil parameters were measured from samples taken during the most recent sampling campaign. Soil texture measurements were only made at 16 sites.

Site name	Plot size (limed/ control) [ha]	Number of times limed	Type of lime †	Lime quantity [Mg ha⁻¹]	ANC‡ [kmol$_c$ ha⁻¹]	Mean annual precip. [mm a⁻¹]	Mean annual temp. [°C]	Elevation [m.asl]	Nitrogen deposition [kg N ha⁻¹ yr⁻¹]	Soil pH (H₂O; 0-5 cm; limed/ control)	Soil base saturation (0-5cm; limed/ control) [%]	Soil texture (30-60 cm; sand / silt / clay) [%]
Beech sites:												
Beerfelden 767A	0.25 / 0.1	2	B, B	1, 1	42	977	8.9	447	14	4.1 / 3.9	30 / 7	70 / 18 / 12
Dassel 4227	0.2 / 0.1435	2	A, B	5, 3	140	1221	7.7	430	19	4.8 / 3.7	30 / 7	50 / 36 / 14
Eutin 402	0.25 / 0.25	2	B, B	3, 3	109	746	8.2	55	22	4.9 / 4.1	67 / 11	n.a.
Göhrde 157	0.25 / 0.25	2	A, B	5, 3	140	733	8.8	100	16	4.6 / 3.7	40 / 11	93 / 4 / 3
Grünenplan 142	0.25 / 0.25	3	B(G), B, B	5, 3, 3	133	920	8.9	260	19	5.2 / 4.1	52 / 15	4 / 73 / 23
Grünenplan 51	0.3 / 0.3	1	B(G)	5	75	920	8.9	330	19	5.7 / 5.0	93 / 73	n.a.
Hess. Lichtenau 2680	0.3 / 0.3	2	B, B	1, 1	41	970	7.3	487	17	4.2 / 4.1	10 / 7	32 / 50 / 18
Jossgrund 2268	0.3 / 0.3	2	B, B	1, 1	41	1050	8.5	385	13	4.7 / 4.3	49 / 16	58 / 30 / 12
Sellhorn 34	0.15 / 0.15	2	A, B	5, 3	148	849	8.9	110	19	4.6 / 4.0	56 / 13	85 / 11 / 4
Oak sites:												
Göhrde 140	0.25 / 0.25	2	A, B	5, 3	140	733	8.8	95	16	4.7 / 4.1	37 / 7	n.a.
Sellhorn 66	0.4 / 0.4	2	A, B	5, 3	140	849	8.9	110	20	4.4 / 4.2	48 / 17	n.a.
Spruce sites:												
Bad Waldsee	4.28 / 5.21	3	A, B	2, 6	171	970	8.6	571	19	5.8 / 3.9	91 / 14	59 / 28 / 13
Beerfelden 767B	0.15 / 0.15	2	B, B	1, 1	42	977	8.9	442	15	3.5 / 3.5	8 / 5	n.a.
Dassel 325	0.2 / 0.1	3	A, B, B	5, 3, 3	140	1221	6.9	390	20	4.4 / 3.8	46 / 5	n.a.
Ellwangen	10.24 / 1.32	3	A, B	3, 6	171	847	8.8	482	16	6.3 / 4.0	92 / 24	64 / 26 / 10
Freudenstadt	7.71 / 3.46	3	A, B	3, 6	171	1516	7.4	748	13	4.6 / 3.7	70 / 6	75 / 16 / 8
Göhrde 155 *	0.25 / 0.25	2	A, B	5, 3	140	733	8.8	80	18	-	-	-
Heidelberg	2.13 / 0.82	3	A, B	3, 6	171	1193	8.8	477	14	6.6 / 3.6	98 / 14	69 / 22 / 9
Herzogenweiler	8.28 / 3.28	3	A,, B	3, 6	171	1203	6.7	909	12	5.9 / 3.8	95 / 5	55 / 24 / 21
Horb	8.35 / 2.27	3	A, B	3, 6	171	969	8.2	623	12	4.7/ 4.1	55 / 32	44 / 36 / 20
Hospital	2.59 / 0.51	3	A, B	3, 6	171	827	8	645	18	5.7 / 3.8	91 / 11	36 / 45 / 19
Lauterberg 2023	0.25 / 0.25	3	D, B, B	1, 3, 3	128	1220	6.1	570	22	4.9 / 4.1	46 / 8	n.a.
Lauterberg 75	0.25 / 0.25	2	D, E	1, 3	131	1454	5.1	790	25	4.4 / 4.3	10 / 5	n.a.
Rantzau 50	0.2217 / 0.25	3	C, B, B	3, 3, 3	140	807	8.4	35	26	3.9 / 3.6	30 / 8	n.a.
Segeberg 244 *	0.25 / 0.25	3	B, B, B	3, 3, 3	109	800	8.3	34	26	-	-	-
Segeberg 517	0.25 / 0.25	3	B, B, B	3, 3, 3	109	844	8.3	20	26	4.1 / 3.7	34 / 11	n.a.
Weithard	1.25 / 0.59	3	A(F), B	3, 6	171	832	8.1	627	16	5.1 / 3.8	80 / 10	35 / 47 / 18
Pine site:												
Göhrde 129	0.25 / 0.25	3	A, B, B	5, 3, 3	140	733	8.8	70	18	4.8 / 4.1	49 / 12	n.a.

112 * Only forest floor layer sampled in this plot; † types of lime: A = Calcium carbonate, B = Dolomite; C = Marl lime, D = Thomas-phosphate, E= Slag lime, F = Potassium sulfate, G = Rock phosphate; ‡ Acid neutralizing capacity

2.2 Soil organic carbon stocks

114   We collected soil and forest floor samples from both limed and control plots from each site at four locations distributed around the plot. Samples were taken from the forest floor (L/O$_f$ and O$_h$) as well

116   as from the mineral soil at four predefined depths (0-5, 5-10, 10-30 and 30-60 cm). Samples of the forest floor and the topsoil (0-30 cm) were taken using a root auger (diameter 8 cm) and samples of

118   the subsoil (30-60 cm) using a gouge auger (diameter 3 cm). At each of the four sampling locations per plot, three samples were taken in close proximity to another for each depth and pooled. Forest floor

120   samples were subsequently oven dried at 60 °C, sieved (2 mm) and ground. Mineral soil samples were oven dried at 40 °C, sieved (2 mm) and also ground. Both forest floor and mineral soil samples were

122   then analyzed for carbon (C) and nitrogen (N) contents using a CN analyzer (Euro EA - CN Elemental Analyzer, HEKAtech GmbH, Wegberg, Germany). Carbonates were measured in soil samples that had

124   a pH (H$_2$O) greater than 6.2. This however consisted of just 21 samples (<2% of the complete dataset), and carbonate contents were a fraction of total soil carbon. Sieved forest floor and mineral soil samples

126   were also analyzed for pH in a 1:2.5 H$_2$O solution and mineral soil samples for exchangeable cations (Ca, Mg, K, Na, Al, Fe, Mn) using an ICP-AES instrument (Thermo Scientific iCAP 7400 Radial, Thermo

128   Scientific, Dreieich, Germany). Base saturation was calculated as percentage exchangeable base cations of the effective cation exchange capacity (ECEC). Soil texture was determined using the pipette

130   method at 16 experiment sites.

    Soil bulk density and the mineral soil dry mass per unit area was determined using a modified version

132   of the Blake and Hartge (1986) core method. Samples were taken at four soil pits per plot for the same respective depths where samples were taken for chemical analysis. Depending on the size and relative

134   abundance of stones observed in the soil profile, different approaches were employed to estimate the bulk density of the soil fine-fraction. Methods and equations are described by König et al. (2014). All

136   samples were oven dried at 105 °C for 48 hours and subsequently weighed. Volumes of coarse fragments were determined using the volume displacement method. For the mineral soil, we

138   calculated the fine earth soil mass per unit area for each respective sampling layer as follows:

    Fine earth mass per unit area = BD * (1-stone content) * d * 10   (1)

140   Where, fine earth soil mass per unit area is in kg m^{-2}, BD is the soil bulk density in g cm^{-3}, stone content is relative volumetric coarse fragment content, d is the thickness (depth) of the sampling horizon in

142   centimeters and 10 is a conversion factor for converting g cm^{-2} to kg m^{-2}.

    The organic layer dry mass per unit area was determined at the same four sampling locations where

144   the samples for the chemical analysis were collected using a root auger (diameter 8 cm). The organic material from within the auger was collected and separated into the two forest floor layers (L/O$_f$ and

146 O_h). Roots and plant debris larger than 2 cm in size were removed from the sample, whereupon samples were oven dried and weighed (König et al., 2014):

148   Organic layer dry mass per unit area = (MH *100) / SA *10   (2)

whereby, organic layer mass per unit area is in kg m^{-2}, MH is the dry mass of the organic layer in grams,
150 and SA is the surface area that was sampled in cm^2, and 10 is a conversion factor for converting to kg m^{-2}. Mineral and forest floor organic carbon stocks were calculated as follows:

152      $$\text{SOC stock } = \frac{OC * MuA}{100}$$ (3)

whereby, SOC stock is in Mg C ha^{-1}, OC is the organic C content in g kg^{-1}, MuA is the mass per unit area
154 in kg m^{-2}, and 100 is a conversion factor for converting to Mg C ha^{-1}.

SOC stocks in the limed plots were corrected for fixed-depth differences incurred because of liming-
156 induced changes in soil bulk density (Figure A2) by using the equivalent soil mass (ESM) approach described by Wendt and Hauser (2013). This approach fits a cubic spline curve of cumulative organic
158 carbon stocks with the corresponding soil mass of the reference profile.

Effects of liming were evaluated using two approaches. First, the difference in soil C stocks between
160 limed and control plots were calculated to assess the relative differences. Second, a chronosequence approach was used to assess temporal changes in soil C stocks using historic data, between 1990 and
162 2019, collected at a subset of the paired experiment sites (forest floor: n = 17, mineral soil: n = 13). Table S1 shows the years when forest floor and mineral soil samples were collected. The change in SOC
164 stocks over time was estimated by calculating the slope of a linear best fit function of the SOC stock values over time. In this analysis, we assumed that soil density did not change during this time and
166 accordingly we used bulk density estimates from the most recent measurement date.

2.3 Short term effects of liming on soil CO_2 and CH_4 fluxes

168 Soil carbon dioxide (CO_2) and methane (CH_4) fluxes were measured at three beech forest sites (Dassel 4227 (DAS 4227), Sellhorn 34 (SEL 34), Göhrde 157 (GOH 157)) in both control and limed plots to assess
170 both short and long-term effects of liming. All three sites were freshly re-limed with an equivalent of 3 Mg $CaCO_3$ ha^{-1} in August-September 2020. Accordingly, the measurements made after these liming
172 events reflect the short-term effects of liming on soil respiration and soil methane fluxes. The soil trace gas fluxes were measured using the vented static chamber method. Round chamber bases (polyvinyl
174 chloride, covering a ground area of 0.07 m^2) were inserted 1–2 cm into the soil surface at four randomly locations within each plot. These chamber bases were covered with polyethylene lid (~22 L headspace
176 volume), from which gas samples were collected at 20-minute intervals for one hour (2, 22, 42 and 62 minutes) and stored in pre-evacuated 12 mL Labco Exetainers® (Labco Limited, Lampeter, UK). To

178   minimize effects from diurnal fluctuations we randomized the order the plots were measured during

each measurement campaign. Gas samples were analyzed using a gas chromatograph (GC, SRI 8610c,

180   SRI Instruments, Torrance, USA), equipped with a flame ionization detector to measure CH_4 and CO_2.

The latter gas species was analyzed by converting it to CH_4, using a built-in methanizer in the GC. The

182   GC was calibrated prior to each analysis using three calibration gases (Deuste Steininger GmbH,

Mühlhausen, Germany), spanning the concentration range of the field samples. Soil gas fluxes were

184   calculated using the ideal gas law, based on the linear increase of gas concentrations in the chamber

over time and corrected with air temperature and atmospheric pressure measured at the time of

186   sampling. A positive flux indicates a net emission, while a negative flux indicates a net consumption.

In parallel to the greenhouse gas flux measurements, we also measured air pressure, soil and air

188   temperature and chamber volume during each measurement.

In early September 2020, we measured soil CO_2 and CH_4 fluxes at one site (DAS 4227) three times in

190   the week prior to lime application (on Sep 7, 2020) to evaluate baseline fluxes and determine whether

there were long-term effects of previous liming events still evident. After liming, we measured GHG

192   fluxes weekly for two months (to Nov. 3, 2020) to evaluate immediate effects of the liming.

Subsequently, in the spring of 2021, we resumed gas flux measurements on a bi-weekly basis at the

194   DAS 4227 site, and additionally also commenced soil GHG measurements at the two other sites (SEL

34, GOH 157). These measurements were made from Mar. 11, 2021 to Jul. 8. 2021.

196   **2.4 Calculation of lime-derived CO_2 emissions**

The proportion of lime-derived CO_2 to the overall CO_2 flux, was determined using $\delta^{13}C$ stable isotope

198   approaches and a two-pool mixing model at the same three sites where soil GHG fluxes were

measured. Unlike the soil GHG measurements, we collected gas samples for $\delta^{13}CO_2$ analysis every

200   second measurement campaign. Samples were collected two minutes and 62 minutes after chamber

closure. The ^{13}C signature of newly formed CO_2 (δ_n) between time point t = 1 (2 minutes; δ_1) and t = 2

202   (62 minutes; δ_2), and the newly formed CO_2 fraction at t = 2 is given by the following mass balance

equation (Martinson et al., 2018):

204    $$\delta_2 = f_n \delta_n + (1 - f_n)\delta_1 \qquad (4)$$

The fraction of lime- derived CO_2 to total CO_2 emissions is calculated following the two-pool mixing

206   model under the assumption that (1) biologically-derived $^{13}CO_2$ is equal between limed and unlimed

plots and (2) CO_2 from lime carbonates and from lime-induced respiration is in isotopic equilibrium:

208    $$f = \frac{(\delta + \delta_0)}{(\delta_1 + \delta_0)} \qquad (5)$$

whereby, δ is the isotopic signature of $^{13}CO_2$ from limed plots, δ_0 the isotopic signatures of $^{13}CO_2$ from

210 unlimed plots, δ_1 the isotopic signature of lime.

The carbon isotope signature ($\delta^{13}C$) of CO_2 was determined by isotope ratio mass spectrometry after

212 gas chromatographic separation, the $\delta^{13}C$ of the added lime was analyzed using an isotope ration mass

spectrometer coupled to an elemental analyzer, both at the Centre for Stable Isotope Research and

214 Analysis (KOSI) at the University of Göttingen.

216 **2.5 Statistical analysis**

Liming effects on SOC stocks at each soil depth were tested using linear mixed effects (LME) models

218 (Crawley, 2013). In these models, the C stock was the response variable, the treatment (control, limed)

was the fixed effect, and the site was the random effect. For the soil trace gas flux measurements, the

220 treatment was considered a fixed effect and the measurement date were considered random effects.

Significance levels were tested separately for each site. Differences were considered significant if

222 $P \leq 0.05$ and marginally significant if $P \leq 0.1$. The input C stock data as well as the output model

residuals were tested for normality using Shapiro–Wilk test. To gain an insight into the underlying

224 factors regulating C stocks in the control (unamended plots) and the relative changes in C stocks as a

result of liming, we used Spearman's rank correlation analyses to assess how C stocks correlated with

226 climatic parameters, stand parameter as well as the inherent soil properties (of the control plot) and

the liming induced changes in soil properties (difference between limed and control plots). The

228 goodness of fit of the non-linear best-fit models were assessed using Pearson correlation analyses

between model-predicted values and measured values. All statistical analyses were carried out using

230 R, version 4.0.02 (R Core Team, 2020).

232 **3. Results**

3.1 SOC stocks in the control plots: magnitude and drivers

234 There was a large variability in SOC stocks across the experimental sites, ranging between 49 and 366

Mg C ha^{-1} (forest floor to 60 cm, in the control plots). In the soil profile, SOC content was highest in the

236 forest floor layer and decreased with soil depth (Figure S1a). In the control plots, 23 % of the total SOC

stock was found in the forest floor layer, 27 % in the topsoil (0-10 cm), and the remaining 50 % was

238 found below 10 cm depth (10-60 cm) (Figure S1b). Soils under coniferous forests stored approximately

38 % more carbon than broadleaf forests (conifer: 157 ± 17 Mg C ha^{-1} (mean ± standard error (SE)),

240 broadleaf: 97 ± 9 Mg C ha^{-1}), where differences were most pronounced in the forest floor L/O$_f$ horizon

and below 10 cm soil depth. Soil bulk density was lowest at the soil surface (0-5 cm) and increased with soil depth. SOC stocks in the mineral soil correlated significantly with soil chemical and physical properties, but not with climatic variables such as temperature, precipitation, or elevation (Table S2). In the forest floor layers, SOC stocks were correlated with both N deposition and pH. For the latter, there was an exponential decrease in the SOC stocks with increasing pH (Figure 1), where, particularly in the L/O$_f$ layer, there was large decline in SOC stocks when pH increased from 3.5 to 4.5. Next, N-deposition exhibited a significant positive correlation with SOC stock in the L/O$_f$ horizon, whereby these effects were only evident in coniferous forests (Figure A3a). This trend was largely driven by the strong linear correlation present between C content and N deposition (Figure A3b), and although the mass of the L/O$_f$ horizon correspondingly increased with N deposition, the most increases were only consistent when N deposition was higher than 25 kg N ha^{-1} yr^{-1} (n = 4) (Figure A3c).
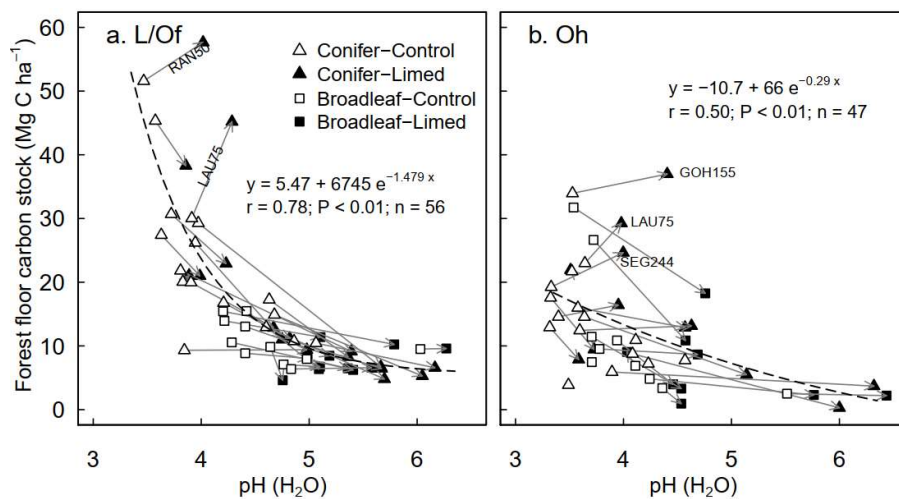
Figure 1: Relationship between the pH of the forest floor layer and the carbon stock of the (a) L/O$_f$ and (b) O$_h$ horizons. The arrows indicate the change from control to limed plots. Missing arrows (in b.) are because the O$_h$ horizon disappeared at those sites as a result of liming. The r is the Pearson correlation coefficients between observed and fitted values. RAN50 is Rantzau 50, LAU75 is Lauterberg 75, GOH155 is the Göhrde 155, SEG 244 is the Segeberg 244 site.

In the mineral soil, SOC stocks correlated with soil texture fractions. This was evident in the significant negative correlations between SOC stock and sand contents at 0-5 cm and 5-10 cm, as well as the positive correlation with clay content at 10-30 cm (Table S2). In the subsoil (30-60 cm), SOC stocks exhibited a similar exponential decay relationship with soil pH as the forest floor layers (data not shown).

3.2 SOC stock response to liming: chronosequence approach

At a subset of experimental sites where historical data were available, most dating back to 1990 (Table S1), forest floor C stocks in the control plots increased in time (0.5 ± 0.1 Mg C ha^{-1} yr^{-1}; Figure 2a), whereby the increases were largely driven by C accumulations at coniferous forest site (0.8 ± 0.3 Mg C

268   ha^{-1} yr^{-1}). Although forest floor SOC stocks in the limed plots also increased over time, the accumulation rates in the L/O$_f$ horizon were significantly lower than the control (Figure 2b). In the mineral soil, there

270   were no significant changes in SOC stocks at any depth during this period. Nevertheless, when C stock change rates were compared between limed and control plots, liming did bolster C accumulation rates
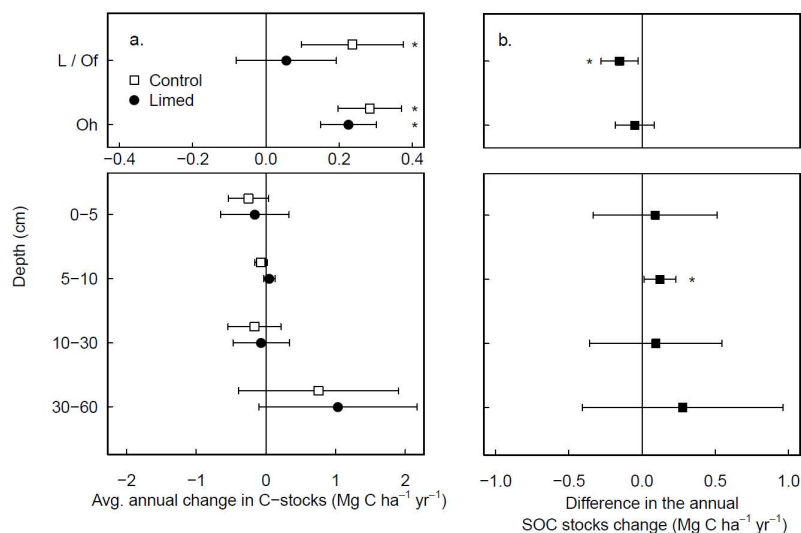
272   slightly at 5-10 cm depth.

274   **Figure 2:** Average (± 95 % T-test-confidence interval) annual changes in SOC stocks experienced over the last two decades in a) both the control and limed plots and b) the difference between the limed

276   and control plots. Statistical significance was tested using LME models for each respective soil depth or layer at P ≤ 0.05 (*).

278

3.3 SOC stock response to liming: paired plot approach

280   Total SOC stocks (forest floor to 60 cm) were comparable between the limed (126 ± 12 Mg C ha^{-1}) and control plots (132 ± 12 Mg C ha^{-1}) (Figure S1b). In the forest floor layer, liming significantly reduced

282   SOC stocks by 34 ± 12 % (equivalent to 8.4 ± 3.6 Mg C ha^{-1}, Figure 3a), which reflects reductions in both C content (-8.8 ± 2.4 %) as well as the forest floor dry mass (-26.1 ± 6.7 %). Both broadleaf and

284   coniferous forests had similar SOC losses in the forest floor layer both in magnitude (broadleaf: -8.1 ± 4.8 Mg C ha^{-1}, coniferous: -8.6 ± 2.7 Mg C ha^{-1}) and in overall proportion of the forest floor SOC
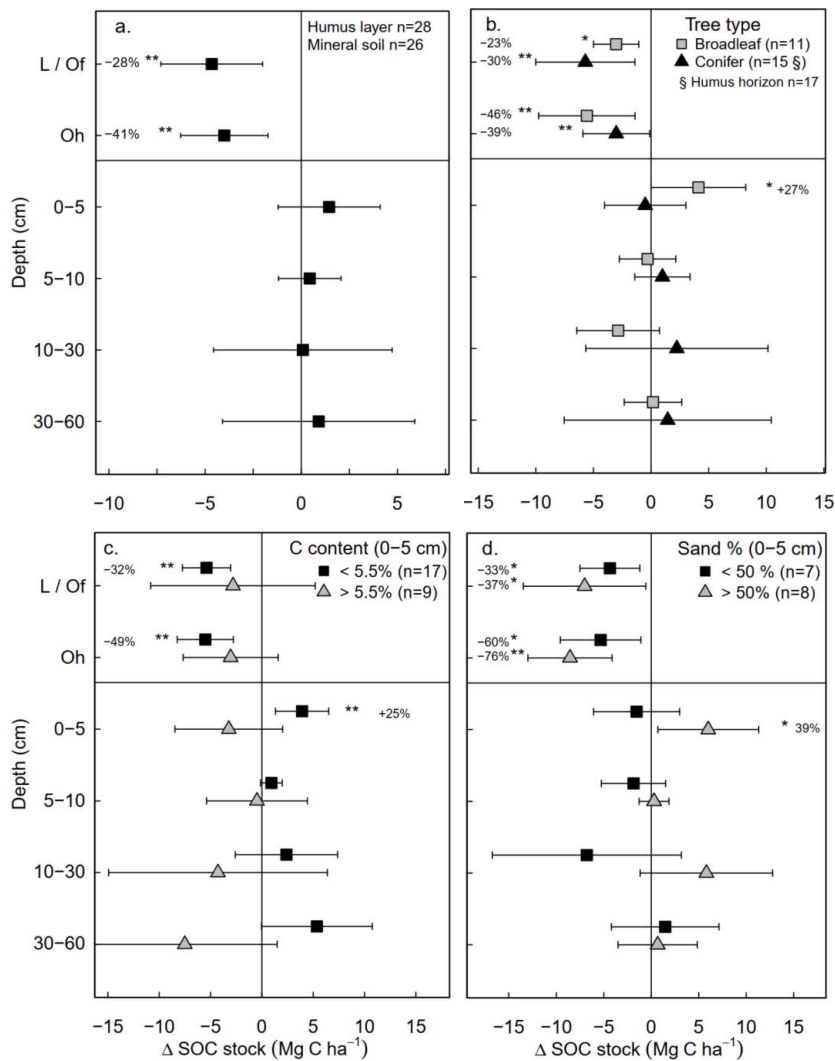
286   stock (Figure 3b).

11

Figure 3: Changes in mean soil organic carbon stock (limed - control) as a result of liming (a) for all plots in the experiment, and classified by (b) tree types and (c) inherent C content of the control plots and (d) site sand percent from 0-5 cm depth. Error bars indicate the 95 % confidence intervals based on Student's T distribution. Statistical significance was tested using LME models for each respective soil depth / layer and grouping at $P \leq 0.05$ (*), and $P \leq 0.01$ (**).

The liming quantities which are responsible for the changes in soil pH, exhibited a negative linear relationship with SOC stock changes (Figure A4), indicating that higher liming dosages result in larger SOC losses. In the forest floor layer, the proportion of C losses or C gains (at a few sites) could further be explained by the initial C stock present on the site (control plot C stock), whereby the C losses were largest at sites with medium amounts of stored C (between 20 and 35 Mg C ha⁻¹), and less pronounced (or even positive) at sites with either little or large C stocks present in the reference state (Figure 4e).
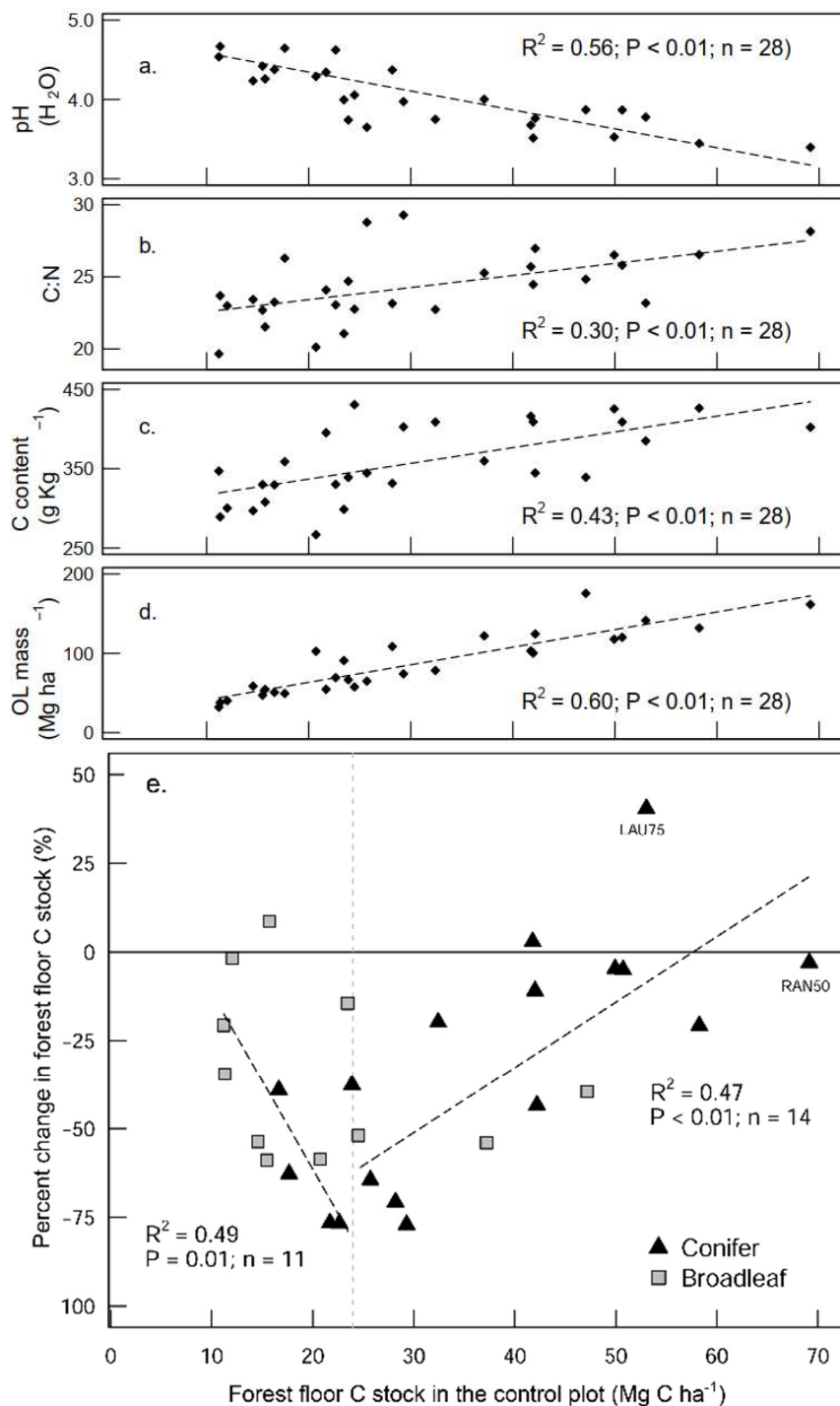
Figure 4: Scatterplot diagrams showing how the forest floor SOC stocks in the control plots relate to a) pH (H_2O), b) the C:N ratio, c) the C content of the forest floor layer and d) the forest floor (organic layer (OL)) biomass. These four parameters show how the forest floor C stock in the control plots are a good measure of organic matter stability. The scatterplot in e) shows the percentage change in the forest floor C stock as a result of liming in relation to the C stocks of the control plots. The two linear regression lines in e) show C change for the different forest floor stock ranges (above and below 25 Mg C ha^{-1}). LAU75 is Lauterberg 75 and RAN50 is Rantzau 50.

Overall, there were no significant changes in mineral SOC stock at any depth (Figure 3a), when all sites are pooled together. Unlike coniferous forests, broadleaf forest plots (n = 11) exhibited significant

increases in SOC stock in the topsoil (0-5 cm) (3.5 ± 1.9 Mg C ha^{-1}, Figure 3b). While it was not significant for SOC stock changes (Table S3), changes in soil C content hinged on the inherent (control) C content (Figure A5). In the mineral soil, the experimental sites that initially had low C contents exhibited increases in C, while sites with already high C contents exhibited decreases. Accordingly, when sites were classified as having either inherently high C contents (>5.5 % at 0-5 cm, n = 9) or inherently low C contents (<5.5 % at 0-5 cm, n = 17), large differences in SOC stocks between the two categories became evident in soil profile (Figure 3c). Namely, SOC stocks increased significantly at sites which inherently had low C contents in the control plots (C content <5.5 % at 0-5 cm, Figure 3c). Here, gains in mineral SOC stocks (0-60 cm) were significantly higher than zero (13.1 ± 4.7 Mg C ha^{-1}), although these gains were partially offset by the SOC losses in the forest floor layers (-10.6 ± 5.6 Mg C ha^{-1}). Conversely, the sites that inherently had high SOC contents in the control plots (C content >5.5 % at 0-5 cm), did not exhibit significant changes in SOC stock at any soil depth throughout the profile, whereby there was a tendency to have SOC losses throughout the profile (forest floor: -5.6 ± 3.5 Mg C ha^{-1}, mineral soil 0-60 cm: -16.4 ± 3.8 Mg C ha^{-1}). Next, SOC stocks significantly increased in the 0-5 cm layer in sandy sites (<50 % sand, Figure 3d), while sites with higher clay and silt fractions exhibited no change in SOC stocks at any depth. In both the forest floor O$_h$ horizon and at 0-5 cm depth, soil C:N ratios decreased significantly as a result of liming (Figure S2).

3.4 Liming effects on soil CO$_2$ and CH$_4$ fluxes in beech forests

The soil greenhouse gas flux measurements made prior to re-liming at the DAS 4227 site (indicative of the long-term effects of liming) showed that (1) there were no significant differences in soil respiration rates between limed and control plots (P = 0.49, Figure 5a), but that (2) methane uptake was twice as high in the limed plots compared to the control (P < 0.01, Figure 5d-f). Immediately following the re-liming, soil CO$_2$ fluxes increased and remained consistently higher than the control (P < 0.01, Figure 5a) for the duration of the measurements. Soil methane uptake on the other hand did not respond to the liming application, and remained consistently lower than the control (P < 0.01 Figure 5d).
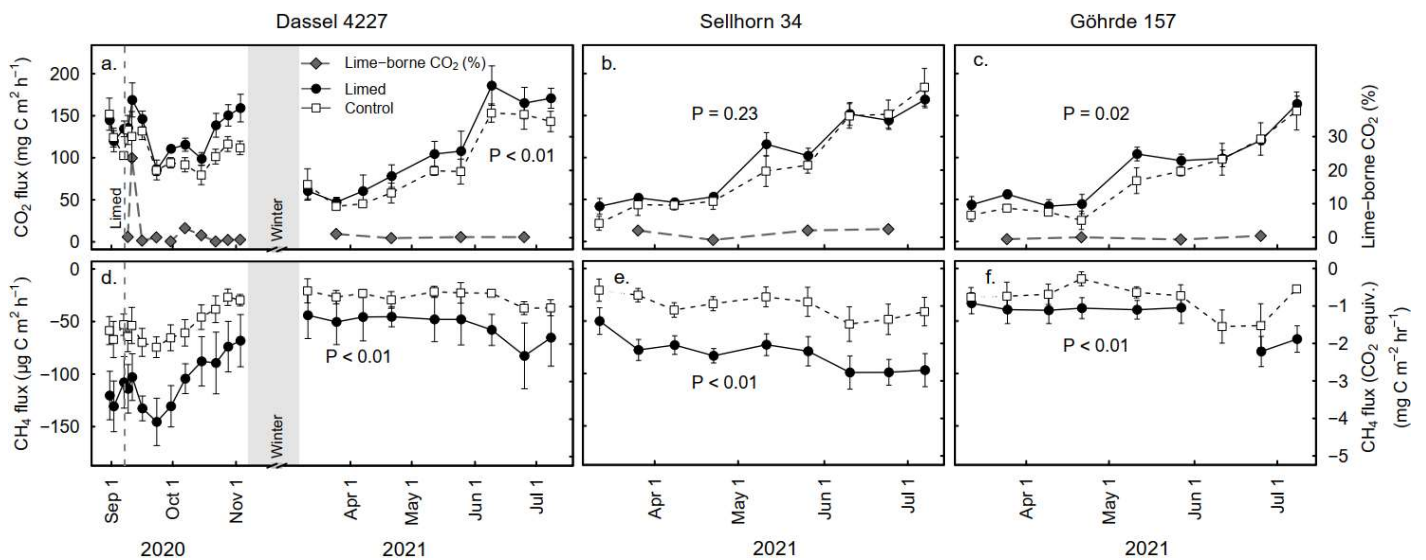
Figure 5: Mean (± SE) soil CO_2 (a-c) and CH_4 fluxes (d-f) at the Dassel 4227, Sellhorn 34 and Göhrde 157 sites in limed and control plots. The grey line in (a-c) indicate the percentage of lime- derived CO_2 of the total CO_2 flux. P-values indicate the significance level between treatments based on LME models. At the Dassel 4227 site, the three baseline measurements made prior to re-liming give an indication of existing long-term differences in soil CO_2 and soil CH_4 fluxes. At time there were no significant treatment differences for CO_2 fluxes (P = 0.49) but CH4 fluxes were significant between the treatments (P < 0.01). At each site 3 Mg $CaCO_3$ ha^{-1} were applied in the late summer of 2020. Soil CH_4 fluxes are presented in both actual measured units and CO_2 equivalence, based on a global warming potential of 28.

Soil respiration measurements made at the beginning of the growing season of 2021 (6 to 10 months after liming) at the three sites (GOH 157, DAS 4227, SEL 34) show that overall soil CO_2 fluxes were significantly higher (23 ± 7 %, P < 0.01) in the limed plots in comparison to the control (Figure 5a-c). The strength of the liming response however depended on the site, where both GOH 157 and DAS 4227 exhibited significant increases in CO_2 fluxes, while the SEL 34 site did not show any significant change in CO_2 flux (Figure 5b). Overall, soil methane uptake was significantly higher in the limed treatments (P < 0.01) and was on average two times higher than the control at all three sites (Figure 5d-f).

Using a stable isotope analysis approach, the overall contribution of lime- derived CO_2 was low, averaging 2.7 % of the total CO_2 flux in the first two months after lime application at the DAS 4227 site. At this site, there was only one short-lived lime-derived CO_2 pulse immediately after a rewetting event five days after liming (Figure 5a) which accounted for 23 % of total (biotic and abiotic) CO_2 emissions. The lime- derived CO_2 contribution remained negligible the following spring when we measured at the three sites, averaging 0.7 ± 0.5 % (n = 3) of the total CO_2 flux.

4. Discussion

4.1 Liming effects on organic C stocks in the forest floor layers

Over the last three decades, forest floor C stocks have gradually been accumulating in both the limed and control plots (Figure 2a), with increases most being pronounced at coniferous sites. These gains likely reflect the influence of elevated N depositions (among other factors) that can (1) enhanced tree growth which accordingly increase litter inputs (Court et al., 2018, Van der Perre et al., 2012) and/or (2) constrain organic matter decomposition rates (Knorr et al., 2005). The effects of N additions were particularly evident at our coniferous forest plots where sites with higher N deposition had larger forest floor carbon accumulations over time (Figure A3).

Considering the biochemical environment plays an intrinsic role in many soil biological processes (Andersson and Nilsson, 2001; Persson et al., 2021; Melvin et al., 2013), changes in soil pH from liming can and will cause a cascade of responses that concomitantly affect the net soil C balance. In the temporal (chronosequence) analysis, the small absolute gains in the forest floor C stocks measured in the limed plots over time (Figure 2a) were significantly lower than those measured in the unlimed control plots (Figure 2b), highlighting how lime applications have (in the majority of sites) promoted organic matter mineralization and offset forest floor OM accumulations. Since overall C stock gains were comparatively minor (in relation to the control), it indicates that lime applications here helped maintain stable organic matter decomposition and nutrient cycling rates.

These results are further substantiated in the paired approach analysis, where a larger number of plots were included (Figure 3a). Although this analysis partly contrast the findings reported by the German National Forest Soil Inventory (which showed that liming decreased forest floor C stocks while unlimed plots remained unchanged over time (Grüneberg et al., 2019)), both of these studies show the same relative trends: namely that liming stimulates organic matter mineralization. This too is corroborated by most other studies (Court et al., 2018; Kreutzer, 1995; Marschner and Wilczynski, 1991; Persson et al., 2021), whereby some publications (Derome et al., 2000; Melvin et al., 2013) have reported the opposite, namely that under certain conditions liming can actually increase soil C stocks.

In this study, we found a clear exponential relationship evident between forest floor C stocks and forest floor layer pH (Figure 1), namely poor sites with acidic pH had high C accumulations in contrast to sites with higher pH that had lower C stocks. In conjunction with increased microbial-induced SOM mineralization, it is also likely that increases in earthworm activity, which is known to increase with liming (Persson et al., 2021), will have assisted the breakup of the litter and the mixing of the organic matter with soil particles and microorganisms throughout the soil layer (Kreutzer, 1995, Persson et al., 2021). Next, the improvements in forest floor composition and morphology were also visually evident at six of the 28 experimental sites, where the humus-form classification improved along the moder to

mull gradient. Similarly, at seven sites, the application of lime meant that the humic horizons (O$_h$)
either did not develop or perhaps were lost over time, indicative of comparatively faster organic matter
mineralization rates and/or earthworm bioturbation. Next, there was also an additive effect of the
lime quantity on C stock, where higher lime applications translated to larger differences in C stocks
with the limed plots (Siepel et al., 2019, Figure A4).

The proportional net change in forest floor C stocks, either C losses or C gains (which were observed
at a few plots) could best be explained when put in the context of the C stock present in the control
plot. This is because the inherent forest floor C stock (in the control plots) is a good measure of organic
matter stability showing the integral effect of different biochemical drivers (such as pH and litter
quality) that regulate SOM breakdown. For instance, sites with high C stocks had correspondingly acidic
pHs (Figure 4a), high C:N ratios (Figure 4b), and both high C contents (Figure 4c) and high SOM mass
(Figure 4d). This contrasts those sites with inherently low forest floor C stocks which had higher pH,
low C:N ratios, low C contents and thin organic matter layers. When we use the C stock of the control
plots as a measure of carbon bioaccumulation, we see that liming effects on forest floor C stocks are
most pronounced at sites with intermediate amounts of carbon (18-35 Mg C ha^{-1}), and less prominent
at the other ends of the index (Figure 4e). First, liming additions to sites which had inherently low
forest floor C stocks (characterized by thin SOM layers and high pH) exhibited only small proportional
losses in overall C stocks (Figure 4e). This minor response is because these sites already had relatively
high pH values and the addition of lime did not change the biogeochemical environment dramatically,
and accordingly there were no large changes in forest floor C stocks. Next, further along this carbon
accumulation gradient, sites with intermediate amounts of carbon exhibited large C losses (up to 75 %
decreases). This is because the application of lime improved the biochemical environment for
microbial communities thereby stimulating organic matter decomposition, which led to strong C losses
at these sites. Finally, sites which have inherently high forest floor C stocks, the application of lime
had an increasingly muted effect on C losses, ultimately leading to negligible changes in C stocks, and
even gains at some sites (for example LAU75). Sites at this end of the spectrum were particular poor,
having inherently low pH and thick organic horizons. Here we suspect that more lime had to be applied
in order to buffer soil acidification in an extent that leads to pH improvements favorable for soil
microorganisms and other soil biota. Thus, microbial activity and accordingly also decomposition rates
remained more or less unchanged. We suspect that the inherent biochemical conditions at this end of
the spectrum are likely similar to those reported by Melvin et al. (2013) in hardwood forests in the USA
and by Derome et al. (1990, 2000) in spruce and pine stands in Finland, who both report significant
gains in SOC stocks as a result of liming.

4.2 Liming effects on organic carbon stocks in the mineral soil

432   In the mineral soil, liming had a variable response on SOC stocks. In the temporal analysis (Figure 2b) we measured a liming-induced increases in SOC in the topsoil (5-10 cm) over time, similar but less

434   pronounced than those reported by the German National Forest Soil Inventory (Grüneberg et al., 2019). In the paired approach analysis we found that the direction and magnitude of net SOC changes

436   in response to liming at each site hinged on the strength of different processes at each site. These are primarily influenced by the sites' biochemical conditions and forest type (Figure 3b-d). The observed

438   variable response is driven by the dynamic balance in soil carbon accumulation rates, namely organic matter inputs, its stabilization and losses as CO_2 or dissolved organic carbon (Jackson et al., 2017).

440   Considering the broad biophysical spectrum of sites we sampled at, this net C balance (losses versus gains) varied considerably in response to the increases in soil pH and base saturation in the topsoil.

442   Like in the forest floor layer, SOC losses can be attributed to the stimulation of microbial decomposition of organic matter. The direction and magnitude of the liming-induced SOC stock changes in the mineral

444   soil (at all soil sampling depths) could however best be explained by the soil's SOC storage capacity and how much carbon was stored therein. Generally, we found that sites with low inherent soil carbon

446   contents (in the control plots) exhibited SOC increases, while at the other end of the spectrum those sites with inherently high carbon contents, exhibited decreases in SOC (Figure A5). This trend was also

448   observed by van Straaten et al. (2015) after land-use change, and shows that sites with inherently high SOC stocks are more vulnerable to SOC losses than sites which initially had little to lose. When we

450   separated our dataset into "carbon rich" (SOC content > 5.5 % at 0-5 cm depth) and "carbon poor" sites (SOC content < 5.5 %) we recorded significant increases in SOC stocks in those sites which initially

452   had low carbon (Figure 3c), but no significant change for sites with initially high SOC stocks. The lack of a significant response in this case likely reflects that we did not sample many sites with inherently high

454   soil carbon. Considering the "carbon-poor" sites mostly had high sand content and low soil fertility, the corresponding SOC increases after liming likely reflect a re-equilibration of the ecosystem carbon

456   cycling dynamics (Figure 3d). We suspect, that C stocks were initially depleted at these sites because sustained acidification over decades which will likely have constrained aboveground net primary

458   productivity, which accordingly reduced C inputs into the soil. Subsequent improvements in nutrient availability and reduced Al toxicity as a result of liming likely improved tree growth (Court et al., 2018,

460   Van der Perre et al., 2012), which in turn increased C inputs into the soil. These suppositions are supported by Grüneberg et al. (2019), who similarly report that liming led to high C accumulations at

462   sites with low clay contents, and C losses at sites with high clay contents.

       Next, improvements in both the biochemical environment and litter palatability will likely have

464   stimulated earthworm bioturbation (Persson et al., 2021), as is evident from the higher C-contents measured in the top 5 cm of soil in the limed plots in the broadleaf forest plots (data not shown). . And

466   while earthworm activity is known to promote organic matter mineralization (Lubbers et al., 2017), they also foster the stabilization of physico-chemically protected carbon in soil aggregates by building

468   up mineral-protected microbial necromass (Angst et al., 2019). It is also suspected that the decreases in soil bulk densities in the topsoil (Figure A2) are attributed to this intensified earthworm activity in

470   the liming plots, which will have loosened and aerated the soil improving gas diffusion, therein also incorporating SOM from the O_h into the mineral soil. Although the net effect of earthworm activity on

472   SOC stocks may not be clear (Persson et al., 2021), it may offer an insight into why net SOC stocks significantly increased in the topsoil (0-5 cm) in the broadleaf forest sites (Figure 3a) where leaf Ca

474   increased as a result of liming, but not in the coniferous forests where needle Ca did not improve (data not shown). Another possible mechanism for the measured increases is through Ca-SOM bridging.

476   Here, the divalent Ca^{2+} cations bonded on negatively charged organic matter exchange complexes which stabilize the SOM, thereby reducing the dissolution and mobility of the SOM (Kalbitz et al., 2000)

478   and correspondingly also reducing decomposition processes (Grüneberg et al., 2019; Melvin et al., 2013).

480

4.3 Liming effects on soil respiration and soil methane fluxes

482   The comparable soil respiration rates measured in the limed and control plots at the DAS 4227 site prior to a third lime application, highlight that (at least at this site) soil organic matter mineralization

484   rates had equilibrated after liming (done 27 years prior, Figure 5a-c). The third application of lime (in August 2020) consequently elicited a pronounced and prolonged increase in soil respiration rates at

486   all three sites (Rosikova et al., 2019). These increases were primarily driven by biotic sources with only a very minor contribution (<3 %) coming from lime- derived CO_2 (Figure 5a-c). This is in agreement with

488   Biasi et al. (2008) who measured similarly low abiotic CO_2 production in a limed peatland forest in Finland. It is most likely that the resulting improvements in the soil biochemical environment created

490   suitable conditions for microbial populations to mineralize organic complexes, which led to the increased CO_2 production. However, like SOC stock responses to lime application, the size (and

492   duration) of the CO_2 production increase varied for the three sites. Notably, the two sites with thick SOM horizons (SEL 34 and GOH 157) had smaller and also shorter-lived CO_2 flushes than the more

494   fertile site (DAS 4227). This again supports the earlier observations that especially at poorer sites characterized with thick forest floor layers, liming only moderately improves organic matter

496   mineralization rates.

Interestingly, long-term soil CH_4 uptake in the limed plots was more than twice that of the control plot

498   at the Dassel 4227 site (Figure 5b). Although, we did not take baseline measurements at the other two sites, they too had double the CH_4 consumption than their respective control plots after liming. This

500 strong CH_4 consumption corresponds to the findings of Borken and Brumme (1997), who attributed this to the fact that liming improves both the soil structure (Bronick and Lal, 2005, Schack-Kirchner and

502 Hildebrand, 1998) and reduces the forest floor layer thickness, which in turn improves CH_4 diffusion into the soil. Furthermore, it has been shown that methanotroph abundance and activity is optimal at

504 pHs just below 6 (Amaral et al., 1998). Despite these soils being a relatively large CH_4 sink, their CO_2 equivalency (global warming potential) nevertheless is still dwarfed by CO_2 emissions from organic

506 matter mineralization.

508 **5. Conclusions**

We hypothesized that liming would lead to decreases in the forest floor layer C stock and that these C

510 losses would be offset, if not exceeded, by significant gains in SOC stocks in the topsoil. Liming indeed resulted in significant decreases in forest floor SOC stocks, but these losses were only partially offset

512 by small gains made in the mineral soil under certain conditions. However, the question of whether liming enhances forest soil C sequestration is not straight forward. Although there were overall

514 decreases in C stocks in the forest floor, the size of these losses depended on the inherent pH and decomposability of the organic material (before liming). While liming stimulated decomposition at

516 most sites, some poorer quality sites which were characterized by thick organic matter accumulations exhibited either only minor C losses, and in a few plots even C gains. Although there were no significant

518 changes in SOC stocks in the mineral soil as a result of liming, the direction and magnitude of C stock changes here were likewise site-dependent. Specifically, sites with sandy soils and/or inherently low C

520 storage exhibited large increases in SOC stocks as a result of liming, while on the other hand, C rich sites were more predisposed to C losses, suggesting that the SOC stocks here were more vulnerable to

522 decomposition than at sites which had little to lose.

Independent of liming, there is evidence of C accumulation in the forest floor layers over the last few

524 decades (likely a response to elevated N deposition), but liming was able to moderate the amount of C that has become immobilized in the organic matter. Liming-induced increases in mineralization rates

526 seem to last for only a limited amount of time, as seen on the respiration rates of the soil, while the doubling in methane consumption due to liming lasts for several decades. Still, CO_2-emissions dwarf

528 the CH_4-consumption of the soil.

We can conclude that liming has an influence on forest soil organic carbon stocks. The effect is largest

530 in the forest floor, where liming counteracts the observed temporal organic matter accumulation (due to N deposition), thereby reducing nutrient immobilization in the forest floor. In the mineral soil the

532 effect of liming on soil organic carbon stocks in less pronounced, but there are indications that liming

20

promotes some carbon accumulation processes in the topsoil. In total, the implications of liming on

534   forest soil greenhouse gas budgets are small, but highly site-specific.

Appendix A
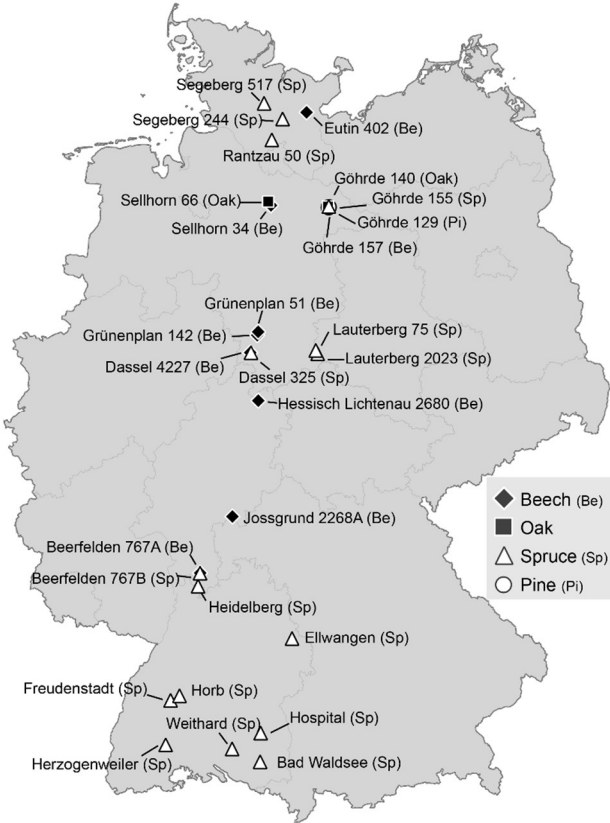
Figure A1: Location of the 28 paired liming experiment sites in Germany where soil organic carbon samples were collected.
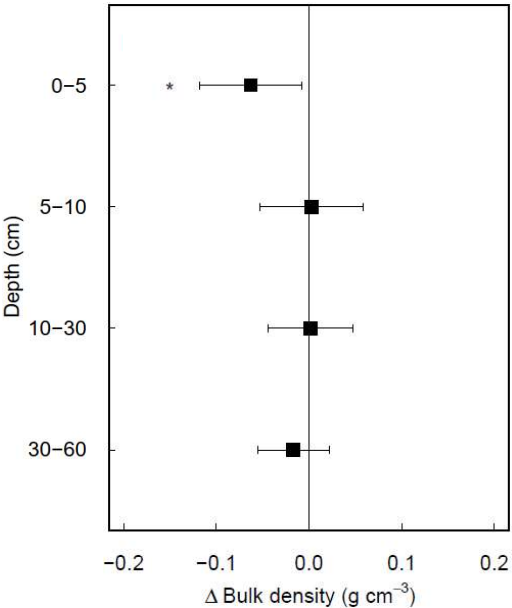
Figure A2: Differences in soil bulk density between limed and control plots. Error bars indicate the 95 % confidence intervals based on Student's T distribution. Statistical significance was tested using LME
models for each respective soil depth / layer at $P \leq 0.05$ (*) and $P \leq 0.01$ (**).
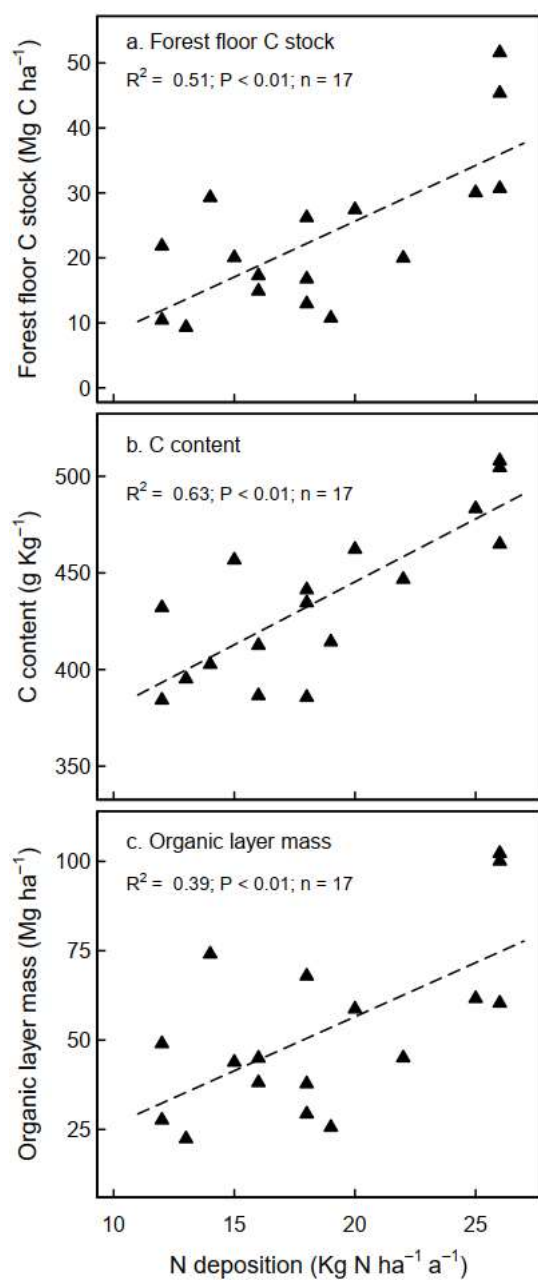
Figure A3: **:** Effects of N deposition on (a) SOC stock (b) C content and (c) dry mass of the L/O$_f$ horizon in unlimed coniferous forests. There was no significant correlation evident with broadleaf forests sites.

550
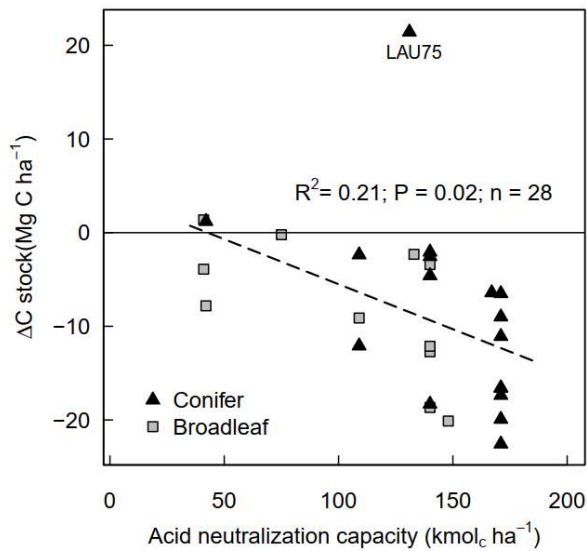
Figure A4: Changes in forest floor C stock (L/O_f and O_h) between limed and control plots in relation to liming quantities, expressed as acid neutralization capacity (ANC). LAU 75 is Lauterberg 75.
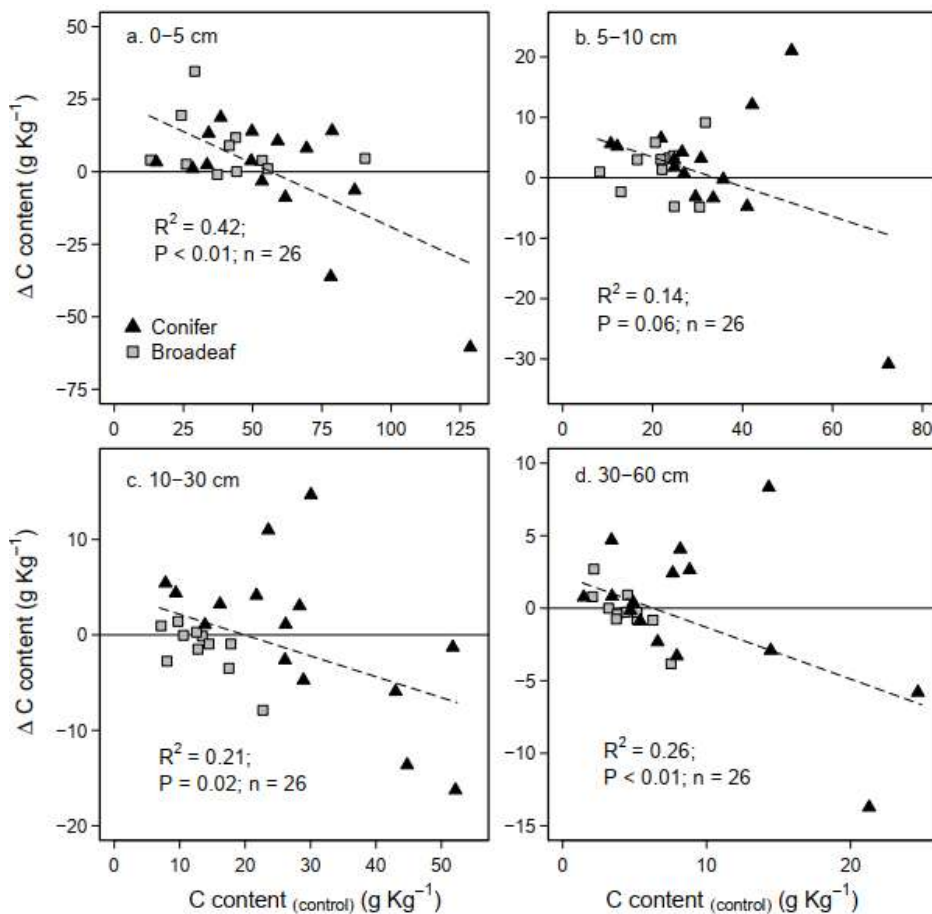
Figure A5: Scatterplot diagrams showing SOC contents in the control plots in relation to the liming-induced changes in SOC contents for the different sampling depths in the soil profile

Author contributions

560

The project was conceptualized by UT and DZ. UT, DZ, LK coordinated the data collection activities and

562 oversaw the maintenance of the liming pairs. GM calculated the lime-derived CO_2 emissions. OvS did

the data analysis and wrote the paper. UT, DZ, LK and GM gave critical feedback on the paper.

564

Competing interests

566 The authors declare that they have no conflict of interest.

578 **References**

Amaral, J. A., Ren, T., and Knowles, R.: Atmospheric Methane Consumption by Forest Soils and
580 Extracted Bacteria at Different pH Values, Applied and Environmental Microbiology, 64, 2397–2402,
https://doi.org/10.1128/AEM.64.7.2397-2402.1998, 1998.

582 Andersson, S. and Nilsson, S. I.: Influence of pH and temperature on microbial activity, substrate
availability of soil-solution bacteria and leaching of dissolved organic carbon in a mor humus, Soil
584 Biology and Biochemistry, 33, 1181–1191, https://doi.org/10.1016/S0038-0717(01)00022-0, 2001.

Angst, G., Mueller, C. W., Prater, I., Angst, Š., Frouz, J., Jílková, V., Peterse, F., and Nierop, K. G. J.:
586 Earthworms act as biochemical reactors to convert labile plant compounds into stabilized soil
microbial necromass, Communications Biology, 2, 441, https://doi.org/10.1038/s42003-019-0684-z,
588 2019.

Biasi, C., Lind, S. E., Pekkarinen, N. M., Huttunen, J. T., Shurpali, N. J., Hyvönen, N. P., Repo, M. E., and
590 Martikainen, P. J.: Direct experimental evidence for the contribution of lime to CO_2 release from
managed peat soil, Soil Biology and Biochemistry, 40, 2660–2669,
592 https://doi.org/10.1016/j.soilbio.2008.07.011, 2008.

Blake, G. R. and Hartge, K. H.: Bulk Density, edited by: Klute, A., Methods of Soil Analysis, 363–375,
594 1986.

Borken, W. and Brumme, R.: Liming practice in temperate forest ecosystems and the effects on CO_2,
596 N_2O and CH_4 fluxes, Soil Use and Management, 13, 251–257, https://doi.org/10.1111/j.1475-
2743.1997.tb00596.x, 1997.

598 Bronick, C. J. and Lal, R.: Soil structure and management: a review, Geoderma, 124, 3–22,
https://doi.org/10.1016/j.geoderma.2004.03.005, 2005.

600 Court, M., Van der Heijden, G., Didier, S., Nys, C., Richter, C., Goutal, N., Saint-Andre, L., and Legout,
A.: Long-term effects of forest liming on mineral soil, organic layer and foliage chemistry: Insights
602 from multiple beech experimental sites in Northern France, Forest Ecology and Management, 409,
872–889, https://doi.org/10.1016/j.foreco.2017.12.007, 2018.

604 Crawley, M. J.: The R Book, Second edition. Chichester, West Sussex, United Kingdom : Wiley, 2013.,
2013.

606 Derome, J.: Effects of forest liming on the nutrient status of podzolic soils in Finland, Water, Air, and
Soil Pollution, 54, 337–350, https://doi.org/10.1007/BF00298677, 1990.

608 Derome, J., Kukkola, M., Smolander, A., and Lehto, T.: Liming of Forest Soils, in: Forest Condition in a
Changing Environment: The Finnish Case, edited by: Mälkönen, E., Springer Netherlands, Dordrecht,
610 328–337, https://doi.org/10.1007/978-94-015-9373-1_39, 2000.

Eklund, L. and Eliasson, L.: Effects of calcium ion concentration on cell wall synthesis, Journal of
612 Experimental Botany, 41, 863–867, https://doi.org/10.1093/jxb/41.7.863, 1990.

Grüneberg, E., Schöning, I., Riek, W., Ziche, D., and Evers, J.: Carbon Stocks and Carbon Stock Changes
614 in German Forest Soils, in: Status and Dynamics of Forests in Germany, vol. 237, edited by:
Wellbrock, N. and Bolte, A., Springer International Publishing, Cham, 167–198,
616 https://doi.org/10.1007/978-3-030-15734-0_6, 2019.

618 Hobbie, S. E., Reich, P. B., Oleksyn, J., Ogdahl, M., Zytkowiak, R., Hale, C., and Karolewski, P.: Tree Species Effects on Decomposition and Forest Floor Dynamics in a Common Garden, Ecology, 87, 2288–2297, https://doi.org/10.1890/0012-9658(2006)87[2288:TSEODA]2.0.CO;2, 2006.

620 Jackson, R. B., Lajtha, K., Crow, S. E., Hugelius, G., Kramer, M. G., and Piñeiro, G.: The Ecology of Soil Carbon: Pools, Vulnerabilities, and Biotic and Abiotic Controls, Annu. Rev. Ecol. Evol. Syst., 48, 419–
622 445, https://doi.org/10.1146/annurev-ecolsys-112414-054234, 2017.

Jansone, L., von Wilpert, K., and Hartmann, P.: Natural Recovery and Liming Effects in Acidified Forest
624 Soils in SW-Germany, Soil Syst., 4, 38, https://doi.org/10.3390/soilsystems4030038, 2020.

Kalbitz, K., Solinger, S., Park, J.-H., Michalzik, B., and Matzner, E.: Controls on the Dynamics of
626 Dissolved Organic Matter in Soils: A Review, Soil Science, 165, 277–304, https://doi.org/10.1097/00010694-200004000-00001, 2000.

628 Knorr, M., Frey, S. D., and Curtis, P. S.: Nitrogen addition and litter decomposition: a meta-analysis, Ecology, 86, 3252–3257, https://doi.org/10.1890/05-0150, 2005.

630 König, N., Blum, U., Symossek, F., Bussian, B., Furtmann, K., Gärtner, A., Groeticke, K., Gutwasser, F., Höhle, J., Hauenstein, M., Kiesling, G., Klingenberg, U., Klinger, T., Nack, T., Stahn, M., Trefz-Malcher,
632 G., and Wies, K.: Handbuch Forstliche Analytik: Eine Loseblatt-Sammlung der Analysemethoden im Forstbereich., Bundesministerium für Verbraucherschutz, Ernährung und Landwirtschaft., Bonn, 678
634 pp., 2014.

Kreutzer, K.: Effects of forest liming on soil processes, Plant and Soil, 168, 447–470,
636 https://doi.org/10.1007/BF00029358, 1995.

Lin, N., Bartsch, N., Heinrichs, S., and Vor, T.: Long-term effects of canopy opening and liming on leaf
638 litter production, and on leaf litter and fine-root decomposition in a European beech (Fagus sylvatica L.) forest, Forest Ecology and Management, 338, 183–190,
640 https://doi.org/10.1016/j.foreco.2014.11.029, 2015.

Long, R. P., Bailey, S. W., Horsley, S. B., Hall, T. J., Swistock, B. R., and DeWalle, D. R.: Long-Term
642 Effects of Forest Liming on Soil, Soil Leachate, and Foliage Chemistry in Northern Pennsylvania, Soil Science Society of America Journal, 79, 1223–1236, https://doi.org/10.2136/sssaj2014.11.0465,
644 2015.

Lubbers, I. M., Pulleman, M. M., and Van Groenigen, J. W.: Can earthworms simultaneously enhance
646 decomposition and stabilization of plant residue carbon?, Soil Biology and Biochemistry, 105, 12–24, https://doi.org/10.1016/j.soilbio.2016.11.008, 2017.

648 Lundström, U. S., Bain, D. C., Taylor, A. F. S., and van Hees, P. A. W.: Effects of Acidification and its Mitigation with Lime and Wood Ash on Forest Soil Processes: A Review, Water, Air and Soil Pollution:
650 Focus, 3, 5–28, https://doi.org/10.1023/A:1024115111377, 2003.

Marschner, B. and Wilczynski, W. A.: The effect of liming on quantity and chemical composition of
652 soil organic matter in a pine forest in Berlin, Germany, Plant and Soil, 137, 229–236, https://doi.org/10.1007/BF00011201, 1991.

654 Martinson, G. O., Pommerenke, B., Brandt, F. B., Homeier, J., Burneo, J. I., and Conrad, R.: Hydrogenotrophic methanogenesis is the dominant methanogenic pathway in neotropical tank
656 bromeliad wetlands., Environ Microbiol Rep, 10, 33–39, https://doi.org/10.1111/1758-2229.12602, 2018.

658   Melvin, A. M., Lichstein, J. W., and Goodale, C. L.: Forest liming increases forest floor carbon and nitrogen stocks in a mixed hardwood forest, Ecological Applications, 23, 1962–1975,
660   https://doi.org/10.1890/13-0274.1, 2013.

Persson, H. and Ahlström, K.: The effects of forest liming on fertilization on fine-root growth, Water,
662   Air, and Soil Pollution, 54, 365–375, https://doi.org/10.1007/BF02385231, 1990.

Persson, T., Andersson, S., Bergholm, J., Grönqvist, T., Högbom, L., Vegerfors, B., and Wirén, A.: Long-
664   Term Impact of Liming on Soil C and N in a Fertile Spruce Forest Ecosystem, Ecosystems, 24, 968–987, https://doi.org/10.1007/s10021-020-00563-y, 2021.

666   R Core Team: R: A language and environment for statistical computing, R Foundation for Statistical Computing, Vienna, Austria, 2020.

668   Reich, P. B., Oleksyn, J., Modrzynski, J., Mrozinski, P., Hobbie, S. E., Eissenstat, D. M., Chorover, J., Chadwick, O. A., Hale, C. M., and Tjoelker, M. G.: Linking litter calcium, earthworms and soil
670   properties: a common garden test with 14 tree species, Ecology Letters, 8, 811–818, https://doi.org/10.1111/j.1461-0248.2005.00779.x, 2005.

672   Rosikova, J., Darenova, E., Kucera, A., Volarik, D., and Vranova, V.: Effect of different dolomitic limestone dosages on soil respiration in a mid-altitudinal Norway spruce stand, iForest -
674   Biogeosciences and Forestry, 12, 357–365, https://doi.org/10.3832/ifor2894-012, 2019.

Schack-Kirchner, H. and Hildebrand, E. E.: Changes in soil structure and aeration due to liming and
676   acid irrigation, Plant and Soil, 199, 167–176, https://doi.org/10.1023/A:1004290226402, 1998.

Shen, Y., Tian, D., Hou, J., Wang, J., Zhang, R., Li, Z., Chen, X., Wei, X., Zhang, X., He, Y., and Niu, S.:
678   Forest soil acidification consistently reduces litter decomposition irrespective of nutrient availability and litter type, Functional Ecology, 35, 2753–2762, https://doi.org/10.1111/1365-2435.13925, 2021.

680   Siepel, H., Bobbink, R., van de Riet, B. P., van den Burg, A. B., and Jongejans, E.: Long-term effects of liming on soil physico-chemical properties and micro-arthropod communities in Scotch pine forest,
682   Biology and Fertility of Soils, 55, 675–683, https://doi.org/10.1007/s00374-019-01378-3, 2019.

Smolander, A., Kitunen, V., Paavolainen, L., and Mälkönen, E.: Decomposition of Norway spruce and
684   Scots pine needles: Effects of liming, Plant and Soil, 179, 1–7, https://doi.org/10.1007/BF00011636, 1996.

686   van Straaten, O., Corre, M. D., Wolf, K., Tchienkoua, M., Cuellar, E., Matthews, R. B., and Veldkamp, E.: Conversion of lowland tropical forests to tree cash crop plantations loses up to one-half of stored
688   soil organic carbon, Proc Natl Acad Sci USA, 112, 9956–9960, https://doi.org/10.1073/pnas.1504628112, 2015.

690   Umweltbundesamt: Nationale Trendtabellen für die deutsche Berichterstattung atmosphärischer Emissionen, Umweltbundesamt, Dessau, 2019.

692   Van der Perre, R., Jonard, M., André, F., Nys, C., Legout, A., and Ponette, Q.: Liming effect on radial growth depends on time since application and on climate in Norway spruce stands, Forest Ecology
694   and Management, 281, 59–67, https://doi.org/10.1016/j.foreco.2012.06.039, 2012.

Wendt, J. W. and Hauser, S.: An equivalent soil mass procedure for monitoring soil organic carbon in
696   multiple soil layers, European Journal of Soil Science, 64, 58–65, https://doi.org/10.1111/ejss.12002, 2013.

698 Xing, K., Zhao, M., Niinemets, Ü., Niu, S., Tian, J., Jiang, Y., Chen, H. Y. H., White, P. J., Guo, D., and Ma, Z.: Relationships Between Leaf Carbon and Macronutrients Across Woody Species and Forest
700 Ecosystems Highlight How Carbon Is Allocated to Leaf Structural Function, Frontiers in Plant Science, 12, 1030, https://doi.org/10.3389/fpls.2021.674932, 2021.

702

704